HYDROLOGICAL PROCESSES
*Hydrol. Process.* **28**, 1573–1586 (2014)
Published online 29 January 2013 in Wiley Online Library
(wileyonlinelibrary.com) DOI: 10.1002/hyp.9694

# Factors influencing long range dependence in streamflow of European rivers

E. Szolgayova,[1]* G. Laaha,[2] G. Blöschl[1,3] and C. Bucher[1,4]

[1] *The Centre for Water Resource Systems, Vienna University of Technology, Austria*
[2] *Institute of Applied Statistics and Computing, University of Natural Resources and Life Sciences, Vienna, Austria*
[3] *Institute of Hydraulic Engineering and Water Resources Management, Vienna University of Technology, Austria*
[4] *Centre of Mechanics and Structural Dynamics, Vienna University of Technology, Austria*

## Abstract:

Investigating long range dependence of river flows, especially in connection with various climate and storage related factors, is important in order to improve stochastic models for long range dependence and in order to understand deterministic and stochastic variability in long-term behaviour of streamflow. Long range dependence expressed by the Hurst coefficient $H$ is estimated for 39 (deseasonalized) mean daily runoff time series in Europe of at least 59 years using five estimators (rescaled range, regression on periodogram, Whittle, aggregated variances, and least squares based on variance). All methods yield estimates of $H > 0.5$ for all data sets. The results from the different estimators are significantly positively correlated for all pairs of methods indicating consistency of the methods used. Correlations between $H$ and various catchment attributes are also analysed. $H$ is strongly positively correlated with catchment area. Apparently, increasing storage with catchment area translates into increasing long range dependence. $H$ is also positively correlated with mean discharge and air temperature and negatively correlated with the mean specific discharge and the seasonality index (maximum Pardé coefficient). No significant correlation is found between the Hurst coefficient and the length of the analyzed time series. The correlations are interpreted in terms of snow processes and catchment wetness. Copyright © 2012 John Wiley & Sons, Ltd.

KEY WORDS catchment attributes correlations; long range dependence; European daily runoff; Hurst coefficient

*Received 22 May 2012; Accepted 18 December 2012*

## INTRODUCTION

The number of large-scale studies analyzing long-term behaviour of streamflows has increased dramatically in the past years. With better data availability and quality and with the rising interest of impact of climate change and climate related factors on streamflow processes (Blöschl and Montanari, 2010), the amount and complexity of these studies have increased. The importance of such research lies in the need of stochastic models incorporating long range dependence, which can be used for example in water resources management or reservoir operations. It is also of interest to relate the long-term behaviour to possible drivers causing these phenomena to understand the most important controls.

There are several ways of considering long-term behaviour of streamflow, both from deterministic and stochastic perspectives. A common method is trend analysis. For example, Petrow *et al*. (2009) conducted a Germany-wide study of flood trends. They found increasing trends in several catchments and a strong dependence of the trends on atmospheric circulation patterns. Stahl *et al*. (2010) found geographically coherent trend patterns of stream flow over Europe which they interpreted by climate drivers. For other large-scale studies examining trends and their relation to external, especially climate related controls, see (Kite, 1989; Kundzewicz *et al*., 2005; Svensson *et al*., 2005; Schmocker-Fackel and Naef, 2010).

Trends are only one phenomenon which is interesting from a long-term perspective. Kite (1989) pointed out, that 'what appears to be a trend now, may turn out to be part of a periodicity when looked at over a longer time span'. Other long-term dependencies of interest are therefore periodic events with frequencies as low as the data permit. Gudmundsson *et al*. (2011), e.g. examined the response of low-frequency components (in terms of relative variance) of runoff to the mean and long-term variations of precipitation and air temperature. They suggest that the low-frequency part of runoff follows atmospheric features but that the low-frequency part of runoff is uncorrelated with the low-frequency components of the climatic factors. However, dependence on catchment properties and mean climatic conditions was found.

Another property characterizing time series from a long-term perspective is the long range dependence (Hurst phenomenon (Hurst, 1951), Hurst–Kolmogorov dynamics or long-term persistence). Here, the autocorrelation function does not disappear even for high temporal lags (Grau-Carles, 2005), or 'correlations decay like a power law' (Doukhan *et al*., 2003). Although this phenomenon has been known for over 60 years, it still

*Correspondence to: Elena Szolgayova, The Centre for Water Resource Systems, Vienna University of Technology, Karlsplatz 13, 1040 Vienna, Austria.
E-mail: szolgayova@waterresources.at

remains largely unexplained and is hotly discussed in the literature. The point of contention is that, if the long range dependence is significant, some of the observed trends should not be interpreted in a causal way. For example, Koutsoyiannis *et al.* (2009) remark on the importance of 'the understanding and modelling of the long-term variability of climatic processes ... with particular emphasis on the Hurst-Kolmogorov dynamics' and the need of communicating this across disciplines. Koutsoyiannis and Montanari (2007) point out that 'the statistical uncertainty is dramatically increased in the presence of dependence, especially if this dependence is long-term persistence' and highlight the need of examining this phenomenon with respect to 'other climatic hypothesis'. Alternatively, Salas *et al.* (1979) considered the Hurst phenomenon as a pre-asymptotic feature, which can be reproduced by appropriate stationary models such as shifting mean models. Long range dependence can be numerically expressed by the Hurst coefficient $H$. This is a coefficient ranging between 0 and 1, where $H > 0.5$ indicates long range dependence in the data (Section 2). There exists a wide range of methods for estimating the Hurst coefficient (an overview can be found for example in Teverovsky *et al.* (1995), both in time and in the frequency domains. Historically, the first method used to estimate $H$ is the rescaled range ($R/S$) analysis. This estimator does not account for short memory in the data nor for heteroscedasticity (Lo, 1991), and it suffers from 'size distortions' for small data sets (Grau-Carles, 2005). Despite the numerous known drawbacks, the rescaled range estimator is a rather popular method used in literature (Lye and Lin, 1994; Sakalauskiene, 2003). There are numerous papers examining estimators for artificially generated data with various properties. Grau-Carles (2005) compares estimators with respect to the length of the time series based on generated ARMA/GARCH series. He observes that the regression on periodogram method (developed by Geweke and Porter-Hudak (1983)) and the detrended fluctuation analysis outperform the other methods (R/S and modified R/S estimator), which often estimates $H > 0.5$ even if the time series was generated from a process without long range dependence. Montanari *et al.* (1999b) generate series from a seasonal ARIMA model, to analyse the effects of periodic components on the $H$ estimates. The Whittle estimator (Beran, 1994) turns out to be the most precise estimator despite the presence of short-term dependencies. The Whittle estimator is a likelihood-based method, which fits a fractionally integrated ARMA model to the data. The quality of the results depends on the correct choice of the underlying model, which might not be trivial. Furthermore, the Whittle estimator assumes normal distribution of the time series, which is usually not the case considering hydrological data. Another method performing well in the tests of Montanari *et al.* (1999b) is the aggregated variances algorithm. A comparison of 12 estimators applied to artificially generated series (using fractional Gaussian noise and fractionally integrated time series) was conducted by Rea *et al.* (2009). They find the Whittle estimator to be among the most accurate methods when distinguishing time series with long memory and those with other non random components. Tyralis and Koutsoyiannis (2011) test 12 methods on generated fractional Gaussian noise series. In this study, three methods estimating both the Hurst coefficient and the variance of the time series simultaneously are included. The authors conclude, that these three methods, a maximum likelihood estimator (McLeod and Hipel, 1978), least squares based on standard deviation (Koutsoyiannis, 2003), and a newly proposed method least squares based on variance (LSV) are 'more accurate' compared to the other methods in test (including the rescaled range, regression on periodogram, the aggregated variances algorithm, and a modification of the Whittle estimator - the local Whittle estimator (Robinson, 1995). Furthermore, according to Tyralis and Koutsoyiannis (2011), the LSV method is computationally faster compared to the LSSD and ML algorithms; thus, it is more suitable for long series of records, which is our case. The above listed studies analyze generated (artificial) time series with chosen properties where clear comparisons of estimated and prescribed Hurst coefficients can be established. However, a comparison can not be made based on real data, whose exact properties are never known.

There are several studies analyzing long range dependence on actual, non-artificial data using different methods. Local scale studies include Radziejewski and Kundzewicz (1997), Montanari *et al.* (1999a), and Zhang *et al.*, (2008), which all detect long range dependence in the discharge data sets.

On a larger scale, Pelletier and Turcotte (1997) conducted a study estimating the Hurst coefficient from average power spectra of monthly discharge data of 636 catchments in the United States and found long range dependence. Koscielny-Bunde *et al.* (2006) conducted a study of 41 series of daily river runoff worldwide using wavelet-based techniques, again having detected long range dependence in the data. Ehsanzadeh and Adamowski (2010) found long range dependence in weekly summer/winter low flows of approximately 200 Canadian stations and noted that long range dependence had strong influence on trend estimation. Lye and Lin (1994) tested long range dependence of peak flow series of 90 Canadian rivers based on rescaled range analysis and concluded there is 'fairly high probability of long-term dependence'. Mudelsee (2007) found $H$ of monthly streamflow to increase along the stream network for four out of six rivers which they explained as a 'result of spatial aggregation of short-memory reservoir contributions in the network'. While there have been numerous studies testing for the presence of long range dependence in streamflow data, very little has been done on analyzing the hydrological controls on the long range dependence. The aim of this paper is therefore to analyze the long-term behaviour of streamflow with respect to possible drivers. Specifically, we address the following questions: What are the Hurst coefficients of mean daily discharge time

 

series of European rivers? Are the estimated Hurst coefficients consistent for various methods? What are the factors influencing the Hurst coefficient in these data? In order to address these questions, we first estimate the Hurst coefficients of discharge time series of European rivers using five different methods and examine the consistency of the results (meaning compare the Hurst coefficient estimates calculated by each of the methods). In a second step, we correlate the Hurst coefficients so obtained with various catchment attributes to find possible drivers of long range dependence.

## METHODOLOGY

### The Hurst coefficient

Long range dependence is numerically expressed by the Hurst coefficient $H \in (0.5, 1]$. In general holds $H \in [0,1]$. For $H = 0.5$, the time series is random noise. For $H < 0.5$, the time series is said to be antipersistent, but this case is rarely of interest in hydrology (Koutsoyiannis, 2005). Processes with long-term persistence have the property of slowly decaying autocorrelation

$$\rho_\tau \sim C\tau^{2H-2} \qquad \tau \to \infty \tag{1}$$

where $\rho_\tau = Corr[X_t, X_{t+\tau}]$ is the autocorrelation function of a weakly stationary time series $X_t, t = 1, 2, \ldots$ with finite variances (Montanari *et al.*, 1999b) and $C$ is a constant (note that stationarity does not exclude the possibility of long memory, because even for high lags, autocorrelation might still depend only on the time lag).

Based on the literature (Montanari *et al.*, 1999b; Koutsoyiannis, 2003; Grau-Carles, 2005; Tyralis and Koutsoyiannis, 2011), five estimators were selected here:

- Rescaled range (R/S),
- Regression on periodogram,
- Whittle estimator,
- Aggregated variances, and
- LSV.

A description of the methods can be found in Appendix B.

The data were deseasonalized prior to the Hurst coefficient estimation. The seasonality in the mean was removed by subtracting a moving average of daily means over 15 days. The seasonality of higher than the first moments was not removed. Denote $X_{i,j}$ a time series, where $i = 1, \ldots, 365$ stands for the days of the year and $j = 1, \ldots, n_y$ represent the years with $n_y = \lceil N/365 \rceil$ the number of years and N the number of days. Then, the daily averages are obtained as $\bar{X}_i = 1/n_y \sum_{j=1}^{n_y} X_{i,j}$ and the applied filter is $F_t = 1/15 \sum_{i=-7}^{7} \bar{X}_{(t \bmod 365)+i}$ (*mod* being the rest after division) with appropriate modifications for values at the beginning and the end ($t < 7$ and $t > N - 7$). Thus, the resulting series is

$$X_t^{(d)} = X_t - F_t \tag{2}$$

### Correlation of Hurst coefficient and catchment attributes

As measures of correlation between the Hurst coefficient estimates and the catchment attributes Spearman's $\rho$ and Kendall's $\tau$ are used. Spearman's $\rho$ estimates how well the dependence between the two considered variables can be expressed by a monotonic function. It is given by

$$\rho = \frac{\sum_{i=1}^{n_{TS}} (h_i - \bar{h})(a_i - \bar{a})}{\left( \sum_{i=1}^{n_{TS}} (h_i - \bar{h})^2 \sum_{i=1}^{n_{TS}} (a_i - \bar{a})^2 \right)^{0.5}} \tag{3}$$

where $h_i$ and $a_i$ are the ranks assigned to the Hurst coefficient estimates and the catchment attributes, respectively. $n_{TS}$ is the total number of the runoff time series analyzed.

Kendall's $\tau$ is based on rank comparison, assessing the number of same ordered pairs of each of the variables:

$$\tau = \frac{n_c - n_d}{0.5 n_{TS}(n_{TS} - 1)} \tag{4}$$

where $n_c$ and $n_d$ are the number of concordant and discordant pairs, respectively. A pair of observations $h_i, a_i$ is concordant if $h_i > a_i$ and discordant for $h_i < a_i$. Both of these correlation measures range between $(-1, 1)$. Values close to zero indicate in both cases that the variables are almost uncorrelated. The calculated values will be given with the result of a statistical test with the null hypothesis $H_0$: The Hurst coefficient and the respective attribute are statistically uncorrelated.

## DATA DESCRIPTION

Time series of mean daily discharges of European rivers were analyzed. The data were provided by the Global Runoff Data Centre (GRDC, 2011) and by the UNESCO FRIEND database.

The character of the analyses requires as long records as possible, otherwise long and short-term dependencies or trends can be difficult to distinguish (Montanari, 2003). In order to maintain relatively uniform spatial coverage of Europe and to minimize estimation uncertainty, only data sets with a minimum length of 59 years were considered. The data were subject to preliminary analysis. The runoffs used in this paper are originating mostly from large rivers; thus, the effect of human interventions (such as urbanization or agriculture) on storage is expected to be small, with prevailing effects of the climate (Blöschl *et al.*, 2007). However, records with evident structural changes, such as shifts in the mean, which may have been due to anthropogenic influences such as dam or reservoir construction, were discarded. Records with missing data were not considered either. A total of 39 streamflow time series remained which are the basis of the analyses in this paper. A brief overview of the dataset, including the number of records per country with the associated time series lengths, is shown in Table I. A more detailed overview including the estimation results, time series length, and catchment areas is given in Table AI. The geographical distribution of the stream gauges is shown in Figure 1.

Table I. Number of stream gauges and streamflow record length by country

| Country | Number of stations | Record lengths (years) |
|---|---|---|
| Austria | 1 | 115–115 |
| Czech Republic | 2 | 88–92 |
| Germany | 10 | 82–159 |
| Denmark | 4 | 96–164 |
| Finland | 1 | 100–100 |
| France | 1 | 128–128 |
| Italy | 4 | 59–68 |
| United Kingdom | 2 | 126–135 |
| Spain | 3 | 63 |
| Switzerland | 2 | 96–98 |
| Norway | 6 | 87–127 |
| Romania | 1 | 150–150 |
| Slovakia | 2 | 94–107 |
| Total | 39 | 59–164 |

The attributes, for which the correlations were estimated, can be divided into two categories. The first group is the catchment characteristics, including climate:

- Log value of the catchment area $logA_i$
- Mean annual air temperature $T_i$ of the catchment area for the respective gauge for the period 1950–2000.
- Mean annual precipitation $P_i$ of the catchment area for the respective gauge for the period 1950–2000.
- Mean elevation $E_i$ of the catchment area

The second group contains runoff related characteristics including record length:

- Log value of the (long-term) mean of daily discharge $log\bar{Q}_i$

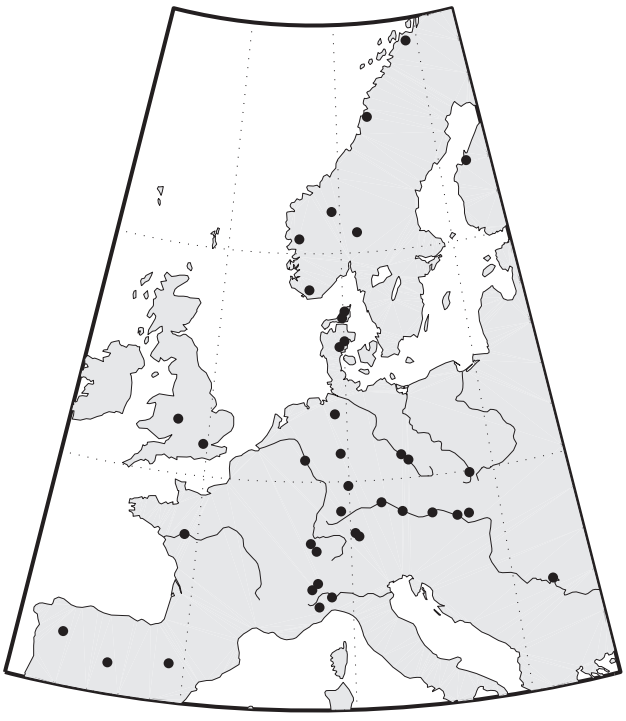

Figure 1. Location of the stream gauges in Europe

- Specific mean discharge $q_i = \bar{Q}_i/A_i$
- Seasonality of monthly flows expressed by the maximum Pardé coefficient (Pardé, 1947)

$$Pk_i = \max_{1\le j\le 12}\left(\frac{12}{N_i}\sum_{l=1}^{N_i}\frac{Q_{jl}^{(i)}}{\sum_{j=1}^{12}Q_{jl}^{(i)}}\right) \quad (5)$$

- where $Q_{lj}$ is the mean monthly runoff for month $j$ and year $l$. This value ranges between 1 and 12. Low values of $Pk_i$ indicate rather uniform distribution of runoff over the year, whereas high values mean stronger presence of seasonal variations in runoff (Parajka *et al.*, 2009).
- Log time series length (in days) $N_i$

Where $i = 1 \ldots 39$ is the index of the station and $N_i$ is the respective series length. The precipitation, elevation and temperature data were obtained from the Catchment Characterization and Modelling database (Vogt *et al.*, 2007).

## RESULTS

### Estimation of the Hurst coefficient

The estimates for each method are shown in Figure 2. On the horizontal axes are the indices of the gauging stations ranked based on the periodogram regression estimation results. The estimated Hurst coefficients range between 0.57 and 1. This means that the analyses indeed suggest long range dependence for all data sets, using any of the methods. The aggregated variance method tends to give the lowest $H$ estimates while the LSV method tends to give the largest $H$ estimates. Indeed, the according to the LSV method $H = 1$ for 21 % of the rivers. Figure 3 shows the $H$ estimates in a geographical context. According to all methods, except LSV, the Hurst coefficients are in general lower in Northern Europe (Norway and Finland) than in Central and Southern Europe. Another geographically consistent group is the four Italian catchments with Hurst coefficient lower than those in Central Europe for all but the aggregated variance method.

The agreement of the estimates is shown in more detail in Figure 4 as a scatter plot of pairs of estimators. In order to assess the degree of agreement of the estimators quantitatively, Kendall's $\tau$ and Spearman's $\rho$ were calculated. The

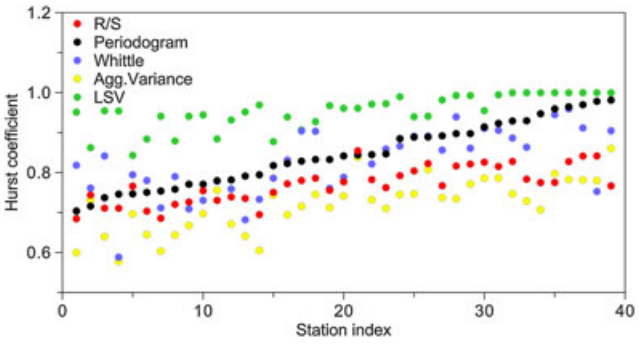


Figure 2. Estimated Hurst coefficients of daily runoff $H$ for all methods. On the horizontal axes are the indices of the runoff time series, ranked in ascending order of $H$ of the periodogram regression method

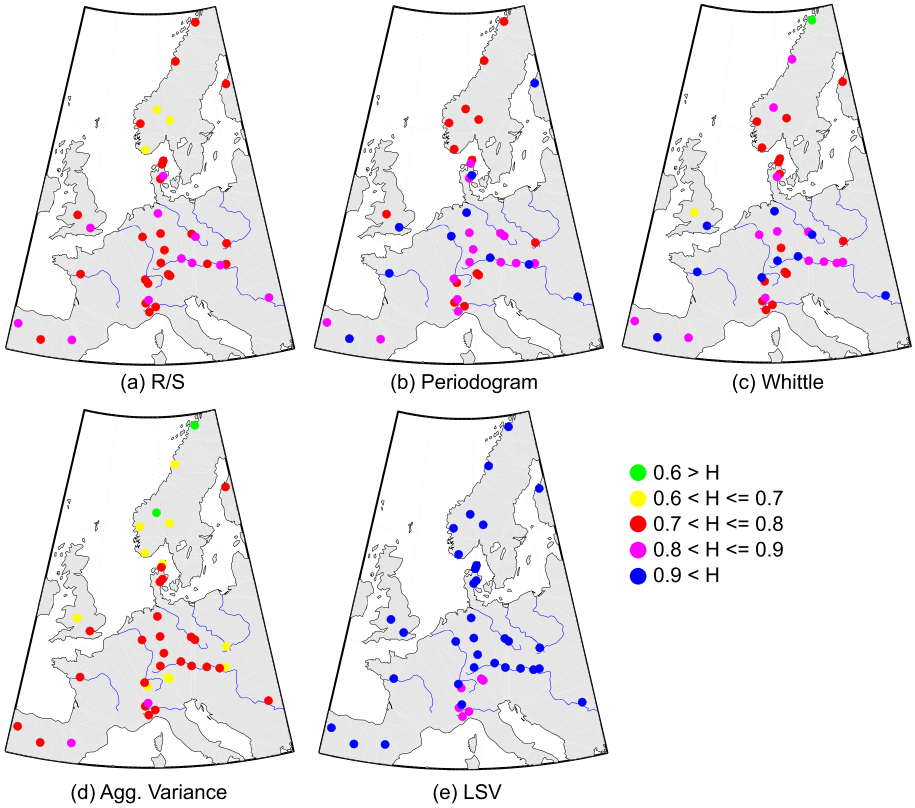


Figure 3. Estimated Hurst coefficients of daily runoff for all estimation methods

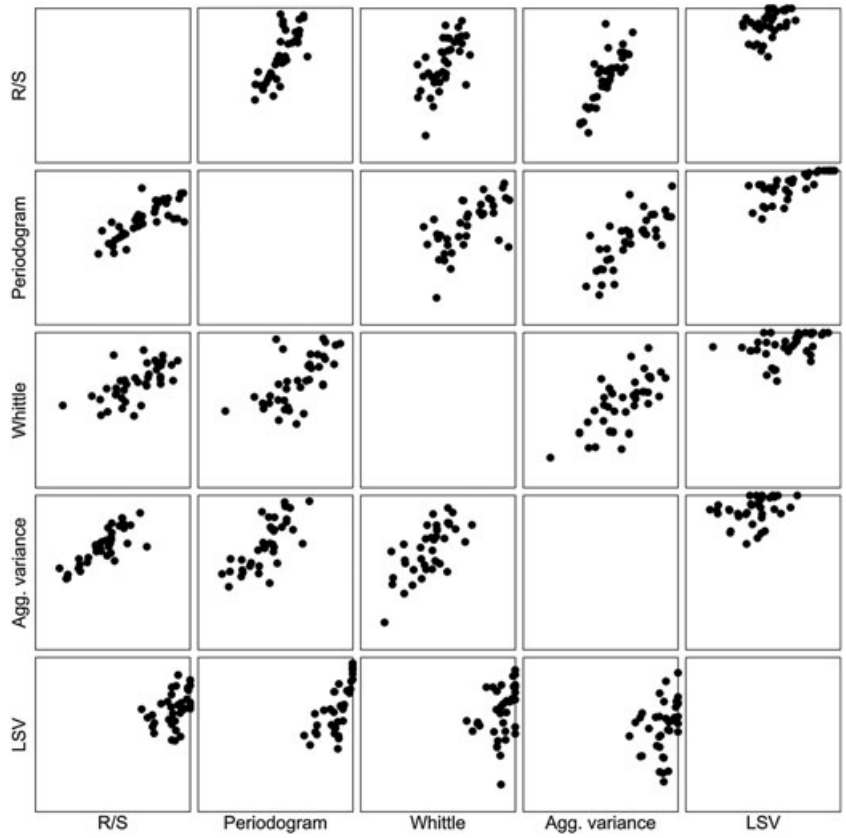


Figure 4. Scatter plots of the Hurst coefficients of daily runoff estimated by different estimation methods. Range of the axes is from 0.5 to 1 in all cases

results are shown in Tables IV and V. All pairs of the estimators show significant positive correlations at the 95% significance level. The highest correlations are obtained between the *R/S* and aggregated variance estimators, and the lowest correlations are obtained between LSV and aggregated variance estimators.

One way of comparing the estimators is calculating the root mean squared error of a respective estimator *est*

$$RMSE^{est} = \left( \frac{1}{n} \sum_{i=1}^{n} \left( H_i^{est} - \bar{H}_{all} \right)^2 \right)^{1/2} \quad (6)$$

where $n$ is the number of data sets and $\bar{H}_{all}$ is the average $H_i$ of all estimators. The $RMSE^{est}$ values are shown in Table II. For R/S, periodogram, and the Whittle estimators, the $RMSE^{est}$ are smaller than 0.06, making the estimators almost equivalent with respect to this measure. LSV and aggregated variances estimates are shifted compared to estimates obtained by the other methods (LSV estimates being generally higher and aggregated variances estimates being lower than the estimation averages), while the remaining estimators are more consistent.

All further evaluations will be done for all estimation procedures. The illustrative figures, however, will be presented for the periodogram method, which has the least RMSE, and the Whittle estimator. The Whittle estimator figures are included since it is possible to estimate confidence intervals for this method to illustrate the uncertainty of the Hurst coefficient estimates. The calculation of the confidence bounds does not incorporate the uncertainties in the estimator assumptions (such as normal distribution); thus, the real confidence bounds would be wider than those calculated as part of the Hurst coefficient estimation.

### Correlation between Hurst coefficient and catchment attributes

Plots of the Hurst coefficient estimated by periodogram regression and the Whittle method against the catchment attributes are shown in Figures 5 and 6. The figures for the two methods are rather similar, which is in accordance with the high correlation between the $H$ of the two estimators (Kendal's $\tau = 0.47$ and Spearman's $\rho = 0.64$; Tables III and IV). In the case of the Whittle estimator, the 95% confidence intervals as described in Appendix B are plotted. The confidence intervals indicate that the correlations are not just an artifact of the sampling uncertainty. Figures 5 and 6 are complemented by calculating Kendall's $\tau$ and Spearman's $\rho$ for all estimation methods and all catchment attributes (Tables V and VI).

The correlations between the Hurst coefficient and the catchment attributes are mostly consistent for all methods of estimation. The least consistent method is LSV which gives somewhat different results for a number of catchment attributes (e.g. seasonality).

Table II. Deviations of the H estimates of daily runoff for each estimation method from the mean of all estimators in terms of root mean squared error

| | R/S | Periodogram | Whittle | Agg. Var. | LSV |
|---|---|---|---|---|---|
| RMSE | 0.058 | 0.042 | 0.047 | 0.107 | 0.137 |
| Estimate mean | 0.77 | 0.85 | 0.82 | 0.72 | 0.95 |

Figure 5 shows an almost linearly increasing dependency between $H$ and catchment area. This effect is not so pronounced when considering the Whittle estimator on Figure 6. However, for all estimation methods, such a positive correlation was tested as significant. Both figures show that $H$ also increases with mean annual air temperature. Indeed, both correlation measures confirm the dependency as significant for all estimation methods except LSV. A decreasing dependence between $H$ and mean annual precipitation $P_i$ can be seen in Figures 5 and 6. However, the significance of this dependence was confirmed only for the periodogram regression and LSV method (for both Kendall's $\tau$ and Spearman's $\rho$). No clear dependence between the Hurst coefficients and elevation can be seen on Figure 6 (the Whittle estimator). A weak decreasing dependence on the elevation can be seen for the periodogram estimator on Figure 5. These graphical results are in accordance with the significance of the correlations measures. Both Kendall's $\tau$ and Spearman's $\rho$ are close to zero ($< 0.07$ in absolute value) for the R/S, Whittle, and aggregated variance estimators. On the other hand, the periodogram and LSV methods show significant correlations between the Hurst coefficient and elevation.

With regards to the runoff-related catchment attributes, a moderate degree of dependence between $H$ and the mean discharge (log) can be seen in Figures 5 and 6 for both methods. This is in accordance with the correlations in Tables V and VI. Unlike for the other catchment attributes, here the two correlation measures give significantly different results. Kendall's $\tau$ ranges between 0.20 and 0.35 (not significant for R/S and aggregated variance) and indicates a lower degree of correlation than Spearman's $\rho$ which ranges between 0.33 and 0.44 where all methods show significant correlations. When the discharge is standardized by the catchment area (specific discharge), the correlations to the Hurst coefficient become more pronounced. The correlations are negative and relatively strong with Spearman's $\rho$ ranging between $-0.40$ and $-0.67$. $H$ slightly decreases with the seasonality expressed as the maximum Pardé coefficient (this coefficient was calculated from nondeseasonalized monthly mean runoffs). This weak to moderate negative correlation is statistically significant for all except the LSV estimator. There is very little correlation between $H$ and the length of the runoff time series with the exception of Spearman's $\rho = 0.21$ for LSV and both correlation coefficients for the aggregated variance ($\tau = 0.23$, $\rho = 0.32$) method. The figures do not show any dependence between the Hurst coefficient and the time series length either.

The correlations described above should be in general interpreted carefully. The correlations do not include information about the actual causality between the runoff and the analyzed climate and storage-based factors. Further interpretation should be made under consideration of the physical processes in the catchment and the correlations between the distinct catchment attributes (see Tables VII and VIII). For example, it can be seen that elevation and precipitation are rather strongly positively

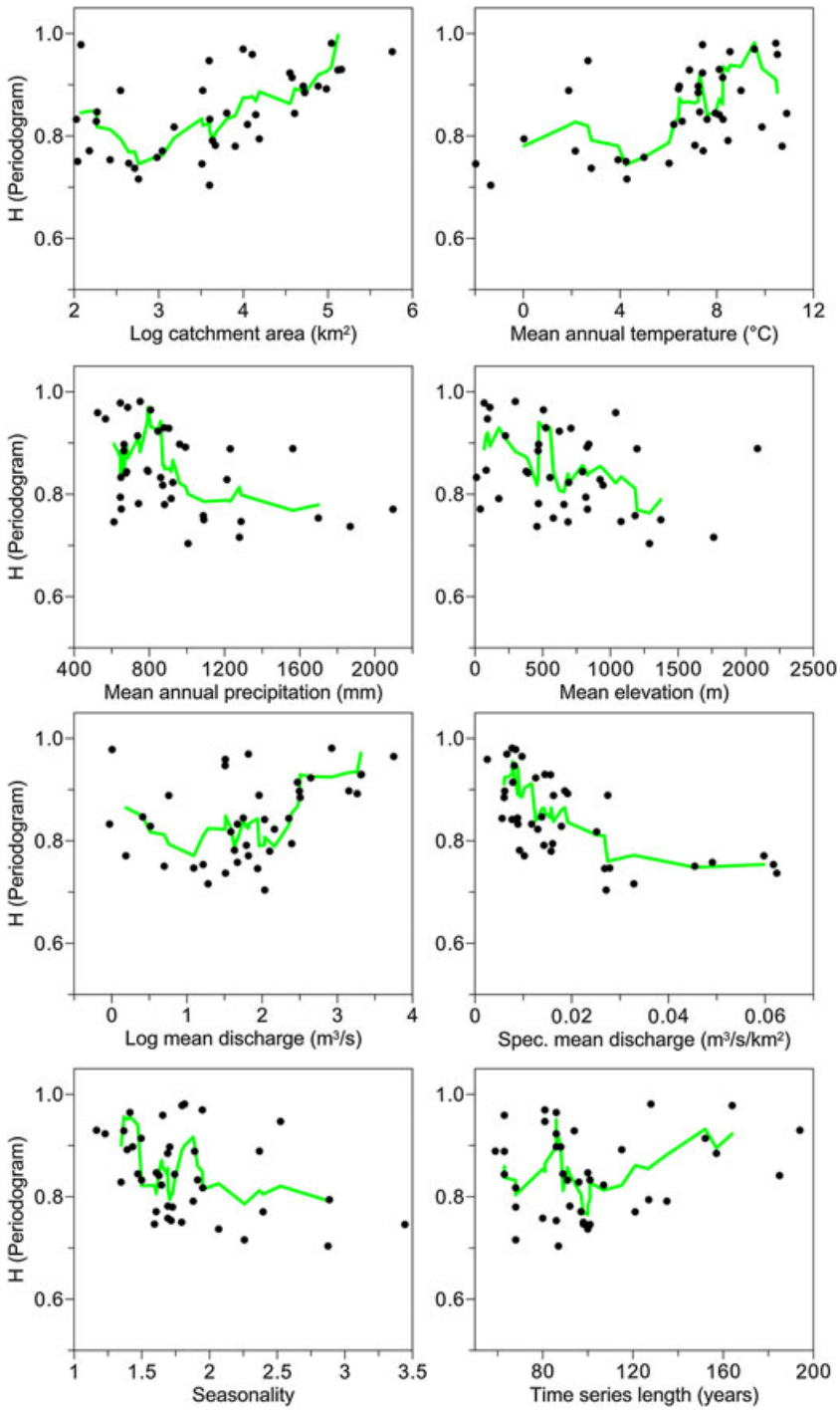


Figure 5. Dependency of the Hurst coefficient of daily runoff (estimated using the regression on periodogram) on catchment area, mean annual air temperature, mean annual precipitation, elevation, mean discharge, specific mean discharge, seasonality of runoff (maximum Pardé coefficient), and the length of the runoff time series. The green line represents a moving average over five data points

correlated; thus, a question arises, whether the long-term dependence in runoff is (partially) caused by elevation, precipitation, or rather the combination of these two factors.

## DISCUSSION AND CONCLUSIONS

The main objective of this study was to analyze correlations between the Hurst coefficient as a measure of long range dependence and various climate and storage-related catchment attributes. As a first step, Hurst coefficients were estimated for 39 European daily river discharge time series. For all estimators, the Hurst coefficients were larger than 0.5. This is in accordance with Koscielny-Bunde *et al.* (2006), another large-scale study analyzing daily discharges, where long range dependence was detected in runoff. When considering those gauges, for which $H$ was estimated in both studies, both Koscielny-Bunde *et al.* (2006) and this analysis find $H > 0.8$ in the majority of cases. The only exception is the Severn at Bewdley, where the estimated values differ by almost 0.2. This may be related to different record lengths in the two studies and different estimation method used. In general, a lower bound

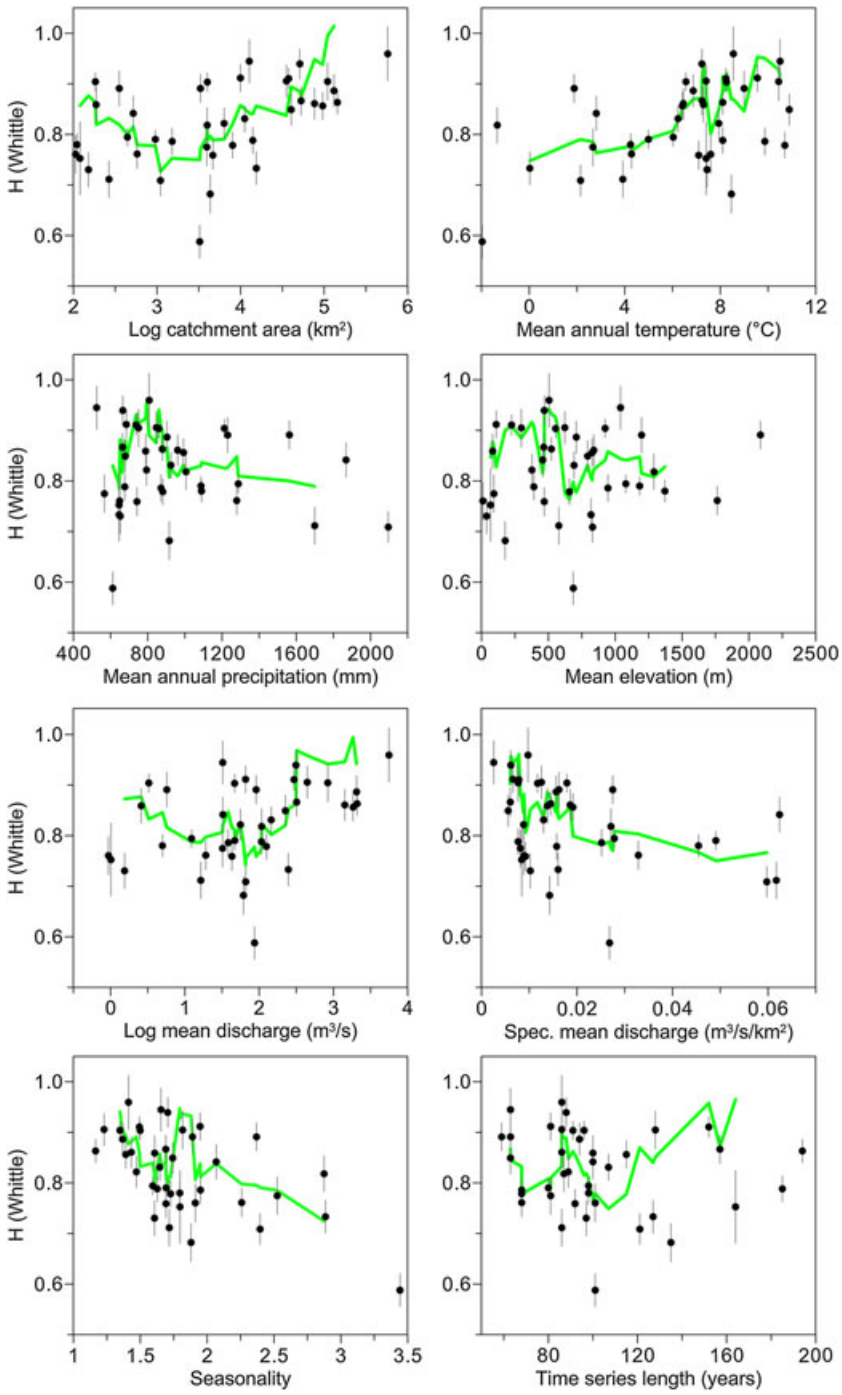


Figure 6. Dependency of the Hurst coefficient of daily runoff (estimated using the Whittle method) on catchment area, mean annual air temperature, mean annual precipitation, elevation, mean discharge, specific mean discharge, seasonality of runoff (maximum Pardé coefficient), and the length of the runoff time series. Bars indicate 95% confidence intervals of *H*. The green line depicts a moving average over five data points

Table III. Kendall's $\tau$ correlations between the Hurst coefficients of daily runoff estimated by different methods

| | R/S | Periodogram | Whittle | Agg. Variances | LSV | Average |
|---|---|---|---|---|---|---|
| R/S | 1.00 | 0.62 | 0.49 | 0.67 | 0.36 | 0.53 |
| Periodogram | 0.62 | 1.00 | 0.47 | 0.56 | 0.65 | 0.58 |
| Whittle | 0.49 | 0.47 | 1.00 | 0.49 | 0.30 | 0.44 |
| Agg. Variance | 0.67 | 0.56 | 0.49 | 1.00 | 0.27 | 0.49 |
| LSV | 0.36 | 0.65 | 0.30 | 0.27 | 1.00 | 0.40 |

Table IV. Spearman's $\rho$ correlations between the Hurst coefficients of daily runoff estimated by different methods

| | R/S | Periodogram | Whittle | Agg. Variances | LSV | Average |
|---|---|---|---|---|---|---|
| R/S | 1.00 | 0.80 | 0.67 | 0.84 | 0.52 | 0.70 |
| Periodogram | 0.80 | 1.00 | 0.64 | 0.76 | 0.81 | 0.75 |
| Whittle | 0.67 | 0.64 | 1.00 | 0.67 | 0.42 | 0.60 |
| Agg. Variance | 0.84 | 0.76 | 0.67 | 1.00 | 0.41 | 0.67 |
| LSV | 0.52 | 0.81 | 0.42 | 0.41 | 1.00 | 0.54 |

Table V. Kendall's $\tau$ correlations between Hurst coefficients of daily runoff and catchment attributes. Those $\tau$, where the independence hypothesis was rejected on a 95% level, are printed in bold. Rightmost column shows the average $\tau$ over all estimation methods

| | R/S | Period. | Whittle | Agg. Var. | LSV | Average |
|---|---|---|---|---|---|---|
| Log catchment area | **0.31** | **0.40** | **0.35** | **0.28** | **0.42** | 0.35 |
| Mean ann. temp. | **0.35** | **0.34** | **0.31** | **0.51** | 0.14 | 0.33 |
| Mean ann. precip. | −0.18 | **−0.30** | −0.04 | −0.15 | **−0.37** | −0.21 |
| Elevation | −0.12 | **−0.26** | −0.04 | −0.02 | **−0.34** | −0.14 |
| Log mean discharge | 0.21 | **0.29** | **0.29** | 0.20 | **0.35** | 0.26 |
| Spec. mean disch. | **−0.43** | **−0.47** | **−0.29** | **−0.38** | **−0.42** | 0.40 |
| Seasonality | **−0.33** | **−0.27** | **−0.35** | **−0.25** | −0.14 | −0.27 |
| Time series length | −0.08 | −0.00 | −0.14 | **−0.23** | 0.15 | −0.06 |

Table VI. Spearman's $\rho$ correlations between Hurst coefficients of daily runoff and catchment attributes. Those $\rho$, where the independence hypothesis was rejected on a 95% level, are printed in bold. Rightmost column shows the average $\rho$ over all estimation methods

| | R/S | Period. | Whittle | Agg. Var. | LSV | Average |
|---|---|---|---|---|---|---|
| Log catchment area | **0.45** | **0.54** | **0.52** | **0.45** | **0.56** | 0.51 |
| Mean ann. temp. | **0.47** | **0.51** | **0.41** | **0.65** | 0.24 | 0.46 |
| Mean ann. precip. | −0.26 | **−0.44** | −0.02 | −0.22 | **−0.56** | −0.30 |
| Elevation | −0.19 | **−0.36** | −0.07 | −0.03 | **−0.50** | −0.21 |
| Log mean discharge | **0.34** | **0.38** | **0.42** | **0.33** | **0.44** | 0.38 |
| Spec. mean disch. | **−0.60** | **−0.67** | **−0.40** | **−0.55** | **−0.60** | −0.57 |
| Seasonality | **−0.45** | **−0.36** | **−0.48** | **−0.34** | −0.20 | −0.37 |
| Time series length | 0.11 | 0.02 | −0.23 | **−0.32** | 0.21 | −0.08 |

Table VII. Kendall's $\tau$ correlations between the catchment attributes. Those $\tau$, where the independence hypothesis was rejected on a 95% level, are printed in bold. $\log(A_i)$ is the log of the catchment area, $T_i$ and $P_i$ are the mean annual temperature precipitation, respectively, $E_i$ is the mean catchment elevation, $\log(\bar{Q}_i)$ and $q_i$ are the log mean and specific discharge, $Pk_i$ is the seasonality expressed by the Pardé coefficient, and $N_i$ is the time series length in years

| | $log(A_i)$ | $T_i$ | $P_i$ | $E_i$ | $log(\bar{Q}_i)$ | $q_i$ | $Pk_i$ | $N_i$ |
|---|---|---|---|---|---|---|---|---|
| Log catchment area | 1 | 0.17 | −0.17 | −0.03 | **0.82** | **−0.31** | **−0.26** | 0.07 |
| Mean ann. temp | 0.17 | 1 | **−0.26** | **−0.24** | 0.05 | **−0.46** | **−0.24** | −0.09 |
| Mean ann. precip | −0.17 | **−0.26** | 1 | **0.45** | −0.03 | **0.64** | −0.03 | −0.13 |
| Elevation | −0.03 | **−0.24** | **0.45** | 1 | 0.05 | **0.43** | 0.07 | **−0.32** |
| Log mean discharge | **0.82** | 0.05 | −0.03 | 0.05 | 1 | −0.13 | −0.19 | 0.08 |
| Spec. mean disch. | **−0.31** | **−0.46** | **0.64** | **0.43** | −0.13 | 1 | 0.12 | −0.07 |
| Seasonality | **−0.26** | **−0.24** | −0.03 | 0.07 | −0.19 | 0.12 | 1 | −0.1 |
| Time series length | 0.07 | −0.09 | −0.13 | **−0.32** | 0.08 | −0.07 | −0.1 | 1 |

for the Hurst coefficient of approximately 0.6 is found in both studies.

Spearman's $\rho$ and Kendall's $\tau$ were used to compare the estimators between each other, obtaining significant positive correlations. This indicates that the estimation results are consistent, even if we cannot verify how far they are varying from the real Hurst coefficients of the data. In order to obtain as realistic results as possible, we deseasonalized the data prior to the analysis, thus avoiding systematic errors which the periodogram and R/S estimators produce in presence of seasonality (Montanari *et al.*, 1999b). The strong correlation between R/S and the periodogram regression ($\tau = 0.62, \rho = 0.80$) is in accordance with an economic study, comparing these two methods on stock returns (Blasco and Santamaría, 1996).

Rather than in the exact value of $H$, we were interested in the strength of the long range dependence compared to those of the other catchments in the study. Since the estimators

Table VIII. Spearman's $\rho$ correlations between the catchment attributes. Those $\rho$, where the independence hypothesis was rejected on a 95% level, are printed in bold. $\log(A_i)$ is the log of the catchment area, $T_i$ and $P_i$ are the mean annual temperature precipitation, respectively, $E_i$ is the mean catchment elevation, $\log(\bar{Q}_i)$ and $q_i$ are the log mean and specific discharge, $Pk_i$ is the seasonality expressed by the Pardé coefficient, and $N_i$ is the time series length in years

| | $log(A_i)$ | $T_i$ | $P_i$ | $E_i$ | $log(\bar{Q}_i)$ | $q_i$ | $Pk_i$ | $N_i$ |
|---|---|---|---|---|---|---|---|---|
| Log catchment area | 1 | 0.30 | −0.24 | −0.04 | **0.94** | **−0.44** | **−0.38** | 0.10 |
| Mean ann. temp. | 0.30 | 1 | **−0.33** | **−0.33** | 0.10 | **−0.63** | **−0.34** | −0.12 |
| Mean ann. precip. | −0.24 | **−0.33** | 1 | **0.58** | −0.05 | **0.80** | −0.04 | −0.18 |
| Elevation | −0.04 | **−0.33** | **0.58** | 1 | 0.08 | **0.59** | 0.11 | **−0.46** |
| Log mean discharge | **0.94** | 0.10 | −0.05 | 0.08 | 1 | −0.19 | −0.29 | 0.14 |
| Spec.mean disch. | **−0.44** | **−0.63** | **0.80** | **0.59** | −0.19 | 1 | 0.23 | −0.11 |
| Seasonality | **−0.38** | **−0.34** | −0.04 | 0.11 | −0.29 | 0.23 | 1 | −0.15 |
| Time series length | 0.10 | −0.12 | −0.18 | **−0.46** | 0.14 | −0.11 | −0.15 | 1 |

gave sufficiently consistent results, it was possible to conduct an analysis of the correlations between Hurst coefficients (indicating the strength of the long range dependence) and the selected catchment attributes.

For this purpose, eight catchments attributes such as area, elevation, precipitation, and temperature were used. For each of them, Spearman's $\rho$ and Kendall's $\tau$ correlations between H and the respective catchment attribute were calculated. The dependencies between the Hurst coefficient and the catchment attributes were mostly consistent for all methods of estimation. The analysis showed that the strength of the long range dependence does not significantly depend on the elevation and time series length. Positive dependence was found for mean discharge, catchment area, and mean annual temperature. On the other hand, long range dependence depends negatively on mean specific discharge, mean annual precipitation, and seasonality. The correlation between mean annual precipitation and the Hurst coefficient was significant only for estimates obtained by two of the applied estimation methods. These results are in general agreement with the results of Gudmundsson *et al.* (2011), who analyze correlations of low-frequency components of runoff. Both studies found significant negative correlations between mean precipitation/mean runoff (standardized by area) and the low-frequency component of runoff (meaning high Hurst coefficients in our case). Positive correlations with air temperature are in accordance with this study as well. The positive correlation with catchment area is in accordance with Mudelsee (2007).

No significant correlation was found between the time series length and the Hurst coefficient. This might imply that the drawbacks of the Hurst coefficient estimation procedures are not due to data scarcity, rather than due to imperfect choice of the estimation method or the unknown properties of the measured runoff.

The hydrological interpretations of the results can be discussed in terms of catchment area effects, catchment wetness, and snow processes. Catchment area effects are reflected by two attributes, catchment area itself and river discharge which are highly correlated with catchment area. The positive correlations of $H$ with both attributes suggest that catchment storage will strongly affect the long range dependence of runoff. One may expect larger storage in larger catchments, both due to groundwater (particularly during low flow periods) and inundations (particularly during flood periods). Indeed, catchment response times tend to increase with catchment area (e.g. Gaál *et al.*, 2012). The long-term component of stream flow variability is relatively more important compared to the short-term component when the Hurst coefficient is high. This may be caused by the large storage capacities of a catchment. To examine this effect in more detail, Figure 7 shows $H$ for five stations at the Danube. There is no clear increasing trend of $H$ with the position in the stream. This may be due to the size and complexity and the number of anthropogenic influences in the Danube basin. Further explanatory factors might be the high correlations between the discharges of the Danube stations.

Catchment wetness effects are reflected by mean annual precipitation and mean specific discharge. The negative correlations of $H$ with both attributes suggest wet catchments exhibit low Hurst coefficients while dry catchments exhibit large Hurst coefficients. Apparently, for wet catchments, the short-term variability is stronger than the long-term variability. In contrast, in dry catchments, there is stronger variability on a long-term scale. This is not surprising for two reasons. Wet catchments tend to have frequent rainfall events without a clear low flow season which increases the short-term variability relative to dry catchments. Also, in dry catchments, the between year variability of streamflow may

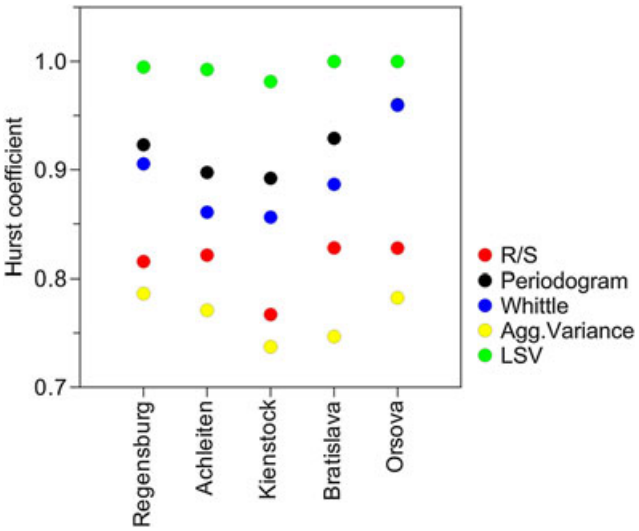


Figure 7. Hurst coefficients of daily runoff for the stations at the Danube River. Stations are ordered according to their position on the river, Regensburg being the closest to the spring of the Danube and Orsova the most downstream of the stations analyzed

be relatively large as runoff is more sensitive to rainfall fluctuations than in wet catchments (Harman *et al*., 2011).

Snow processes are reflected by air temperature and the seasonality index. The positive correlations of $H$ with air temperature and the negative correlations of $H$ with the seasonality (maximum Pardé coefficient) suggest that snow-dominated areas (low air temperature, large seasonal runoff fluctuations, and therefore large seasonality) have less long range dependence (and more short-term fluctuations) than catchments where snow processes are less important. Apparently, a snow-dominated stream flow regimes tends to smooth out the fluctuations between years while there is significant short-term variability that deviates from the mean seasonal variation.

The findings of this study have important implications for stochastic hydrological modelling especially in water resources management and reservoir operation. For example, in order to determine the supply risk from a reservoir, long-term perspective is of interest; thus, the long range dependence needs to be incorporated into the model. This study suggests that, depending on the climate and catchment characteristics, these types of models needed to be parameterised in a different way. From a more theoretical perspective, it is also of interest to identify the main factors related to climate and storage that influence the long range dependence of stream flow at a regional scale.

## ACKNOWLEDGEMENTS

We would like to acknowledge financial support from the Austrian Science Funds (FWF) as part of the Vienna Doctoral Programme on Water Resource Systems (DK-plus W1219-N22). Analyses are based on stream flow data of the EURO-FRIEND-Water archive (EWA) provided under a project specific licence by the Global Runoff Data Centre. We would like to thank Dr. Tyralis and Prof. Koutsoyiannis for providing the Matlab code for the LSV estimator. We would like to thank Prof. Montanari for his valuable advice and inputs. Furthermore, we would like to thank Prof. Kousoyannis and Dr. Tyralis for their helpful review and the anonymous reviewer for his resourceful comments. The feedback from the reviewers helped to improve the manuscript significantly.

## REFERENCES

Beran J. 1994. *Statistics for long - memory processes*. Chapman and Hall: New York.

Blasco N, Santamaría R. 1996. Testing memory patterns in the Spanish stockmarket. *Applied Financial Economics*, **6**: 401–411. DOI: 10.1080/096031096334033

Blöschl G, Montanari A. 2010. Climate change imacts - throwing the dice? *Hydrological Processes* **24**: 374–381. DOI: 10.1002/hyp.7574

Blöschl G, Ardoin-Bardin S, Bonell M, Dorninger M, Gutknecht D, Matamoros D, Merz B, Shand P, Szolgay J. 2007. At what schales do climate variability and land cover change impact on flooding and low flows? *Hydrological Processes* **21**: 1241–1247. DOI: 10.1002/hyp.6669

Doukhan P, Oppenheim G, Taqqu MS. 2003. *Long-range dependence*. Birkhäuser: Boston.

Ehsanzadeh E, Adamowski K. 2010. Trends in timing of low stream flows in Canada: Impact of autocorrelation and long - term persistence. *Hydrological Processes* **24**: 970–980. DOI: 10.1002/hyp.7533

Gaál L, Szolgay J, Kohnová S, Parajka J, Merz R, Viglione A, Blöschl G. 2012. Flood timescales: Understanding the interplay of climate and catchment processes through comparative hydrology. *Water Resources Research* **48**: W04511. DOI: 10.1029/2011WR011509

Geweke J, Porter-Hudak S. 1983. The estimation and application of long memory time series models. *Journal of Time Series Analysis* **40**(4): 221–238. DOI: 10.1111/j.1467-9892.1983.tb00371.x

Grau-Carles P. 2005. Tests of long memory: a bootstrap approach. *Computational Economics* **25**: 103–113. DOI: 10.1007/s10614-005-6277-6

GRDC 2011. *Global Runoff Data Center - Dataset of river discharge time series*. Koblenz: Germany.

Gudmundsson L, Tallaksen LM, Stahl K, Fleig AK. 2011. Low - frequency variability of European runoff. *Hydrology and Earth System Sciences* **15**: 1706–1727. DOI: 10.5194/hessd-8-1705-2011

Harman CJ, Troch PA, Sivapalan M. 2011. Functional model of water balance variability at the catchment scale: 2. Elasticity of fast and slow runoff components to precipitation change in the continental united states. *Water Resources Research* **48**: W02523. DOI: 10.1029/2010WR009656

Hurst HE. 1951. Long-term storage capacity of reservoirs. *Transaction of the American Society of Civil Engineers* **116**: 770–779.

Kite G. 1989. Use of time series analysis to detect climatic change. *Journal of Hydrology* **111**: 259–279. DOI: 10.1016/0022-1694(89)90264-3

Koscielny-Bunde E, Kantelhardt JW, Braun P, Bunde A, Havlin S. 2006. Long - term persistence and multifractality of river runoff records: Detrended fluctuation studies. *Journal of Hydrology* **322**: 120–137. DOI: 10.1016/j.jhydrol.2005.03.004

Koutsoyiannis D. 2003. Climate change, the Hurst phenomenon, and hydrological statistics. *Hydrological Sciences Journal* **48**: 3–24. DOI: 10.1623/hysj.48.1.3.43481

Koutsoyiannis D. Hydrological Persistence and the Hurst Phenomenon. In *The Encyclopedia of Water, Volume 4: Surface and agricultural Water*, Lehr JH, Keeley J (eds). Wiley: New York, 2005; 210–221. DOI: 10.1002/047147844X.sw434

Koutsoyiannis D. 2010. HESS opinions - a random walk on water. *Hydrology and Earth System Sciences* **14**: 585–601. DOI: 10.1175/1525-7541(2003)004<0489:MTDOLV>2.0.CO;2

Koutsoyiannis D, Montanari A. 2007. Statistical analysis of hydroclimatic time series: Uncertainty and insights. *Water Resources Research* **43**. DOI: 10.1029/2006WR005592

Koutsoyiannis D, Montanari A, Lins HF, Cohn TA. 2009. Discussion of 'The implications of projected climate change for freshwater resources and their management'. *Hydrological Sciences Journal* **540**(2): 394–405. DOI: 10.1623/hysj.54.2.394

Kundzewicz WZ, Graczyk D, Maurer T, Pińskwar I, Radziejewski M, Svensson C, Szwed M. 2005. Trend detection in river flow series: 1. Annual maximum flow. *Hydrological Sciences Journal* **500**(5): 797–810. DOI: 10.1623/hysj.2005.50.5.797

Lo A. 1991. Long term memory in stock market prices. *Econometrica* **59**: 1279–1313. DOI: 10.2307/2938368

Lye LM, Lin Y. 1994. Long - term dependence in annual peak flows of Canadian rivers. *Journal of Hydrology* **160**: 89–03. DOI: 10.1016/0022-1694(94)90035-3

McLeod AI, Hipel K. 1978. Preservation of the rescaled adjusted range. 1. A reassessment of the Hurst phenomenon. *Water Resources Research* **140**(3): 491–508. DOI: 10.1029/WR014i003p00491

Montanari A. Long - range dependence in Hydrology. In *Theory and applications of long - range dependence*, Doukhan P, Oppenheim G, Taqqu MS (eds). Birkhäuser: Boston, 2003; 461–472.

Montanari A, Rosso R, Taqqu MS. 1997. Fractionally differenced ARIMA models applied to hydrologic time series: Identification, estimation, and simulation. *Water Resources Research* **33**: 1035–1044. DOI: 10.1029/97WR00043

Montanari A, Longoni M, Rosso R. 1999a. A seasonal long - memory stochastic model for the simulation of the daily river flows. *Physics and Chemistry of Earth (B)* **4**: 319–324. DOI: 10.1016/S1464-1909(99)00007-6

Montanari A, Taqqu MS, Teverovsky V. 1999b. Estimation of long range dependence in the presence of periodicity: An empirical study. *Mathematical and Computer Modelling* **29**: 217–228. DOI: 10.1016/S0895-7177(99)00104-1

Mudelsee M. 2007. Long memory of rivers from spatial aggregation. *Water Resources Research* **430**: W01202. DOI: 10.1029/2006WR005721

Parajka J, Kohnová S, Merz R, Szolgay J, Hlavčová K, Blöschl G. 2009. Comparative analysis of the seasonality of hydrological characteristics in Slovakia and Austria. *Hydrological Sciences Journal* **540**(3): 456–473. DOI: 10.1623/hysj.54.3.456

Pardé M. 1947. *Fleuves et rivierès 2. ed. rev. et corr*. Colin: Paris.

Pelletier JD, Turcotte DL. 1997. Long-range persistance in climatological and hydrological time series: Analysis, modeling and application to drought hazard assessment. *Journal of Hydrology* **203**: 198–208. DOI: 10.1016/S0022-1694(97)00102-9

 

Petrow T, Zimmer J, Merz B. 2009. Changes in the flood hazard in Germany through changing frequency and persistence of circulation patterns. *Natural Hazards and Earth Systems Sciences* **9**: 1409–1423. DOI: 10.5194/nhess-9-1409-2009

Radziejewski M, Kundzewicz ZW. 1997. Fractal analysis of flow of the river Warta. *Journal of Hydrology* **200**: 280–294. DOI: 10.1016/S0022-1694(97)00024-3

Rea W, Oxley L, Reale M, Brown J. 2009. Not all estimators are born equal: the empirical properties of some estimators of long memory. Mathematics and Computers in Simulation, forthcoming.

Robinson PM. 1995. Gaussian semiparametric estimation of time series with long - range dependence. *The Annals of Statistics* **23**: 1630–1661.

Rosse O. February 1996. Estimation of the Hurst parameter of long- range dependent time series. Research Report Series 137, University of Würzburg.

Sakalauskiene G. 2003. The Hurst phenomenon in hydrology. *Environmental Research, Engineering and Management* **3**: 16–20.

Salas JD, Boes DC, Pegram GGS, Yevjevich V. 1979. The Hurst phenomenon as a preasymptotic behavior. *Journal of Hydrology* **4**: 1–15. DOI: 10.1016/0022-1694(79)90143-4

Schmocker-Fackel P, Naef F. 2010. Changes in flood frequencies in Switzerland since 1500. *Hydrology and Earth System Sciences* **14**: 1581–1594. DOI: 10.5194/hess-14-1581-2010

Stahl K, Hisdal H, Hannaford J, Tallaksen LM, van Lanen HAJ, Sauquet E, Demuth S, Fendekova M, Jódar J. 2010. Streamflow trends in Europe: Evidence from a dataset of near - natural catchments. *Hydrology and Earth System Sciences* **14**: 2367–2382. DOI: 10.5194/hess-14-2367-2010

Svensson C, Kundzewicz WZ, Maurer T. 2005. Trend detection in river flow series: 2. Flood and low-flow index series. *Hydrological Sciences Journal* **500**(5): 811–824. DOI: 10.1623/hysj.2005.50.5.811

Taqqu MS, Teverovsky V. 1998. On estimating the intensity of long-range dependence in finite and infinite variance time series. In *A practical guide to heavy tails*, Adler RJ (ed.) Birkhäuser: Boston; 177–217.

Teverovsky V, Taqqu MS, Willinger W. 1995. Estimator for long-range dependence: An empirical study. *Fractals* **30**(4): 785–798. DOI: 10.1016/S0895-7177(99)00104-1

Tyralis H, Koutsoyiannis D. 2011. Simultaneous estimation of the parameters of the Hurst - Kolmogorov stochastic process. *Stochastic Environmental Research and Risk Assessment* **25**: 21–33. DOI: 10.1007/s00477-010-0408-x

Vogt JV, Soille P, de Jager A, Rimaviciute E, Mehl W, Foisneau S, Bódis K, Dusart J, Paracchini ML, Haastrup P, Bamps C. A pan-European River and Catchment Database. Report EUR 22920 EN, EC-JRC, Luxembourg, 2007. URL http://ccm.jrc.ec.europa.eu/php/index.php?action=view&id=23. Web accessed November 2011. DOI: 10.2788/35907

Zhang Q, Xu C-Y, Chen YD, Yu Z. 2008. Multifractal detrended fluctuation analysis of streamflow series of the Yangtze River basin, China. *Hydrological Processes* **22**: 4997–5003. DOI: 10.1002/hyp.7119

## APPENDIX A. DATA AND ESTIMATION RESULTS OVERVIEW

Table AI. Description of the runoff data used in this study, including the Hurst coefficient estimates from all five methods. $N_i$ is the time series length (years), $A_i$ is the catchment area ($km^2$), and $P_i$ is the mean annual precipitation (mm)

| | | | | | | Hurst coefficient | | | | |
|---|---|---|---|---|---|---|---|---|---|---|
| River | Station | Country | $N_i$ | $A_i$ | $P_i$ | R/S | Period. | Whittle | A.Var. | LSV |
| Arhus A | Skibby | DK | 164 | 120 | 646 | 0.84 | 0.98 | 0.75 | 0.78 | 1 |
| Birse | Moutier La Charrue | CH | 96 | 183 | 1213 | 0.78 | 0.83 | 0.9 | 0.72 | 0.91 |
| Cabe | Rivas Altas | ESP | 63 | 353 | 1230 | 0.8 | 0.89 | 0.89 | 0.75 | 0.94 |
| Danube | Achleiten | DE | 86 | 76 653 | 961 | 0.82 | 0.9 | 0.86 | 0.77 | 0.99 |
| Danube | Bratislava | SK | 94 | 131 331 | 904 | 0.83 | 0.93 | 0.89 | 0.75 | 1 |
| Danube | Kienstock | AT | 115 | 95 970 | 992 | 0.77 | 0.89 | 0.86 | 0.74 | 0.98 |
| Danube | Orsova | RO | 150 | 576 232 | 807 | 0.83 | 0.96 | 0.96 | 0.78 | 1 |
| Danube | Regensburg | DE | 86 | 35 399 | 846 | 0.82 | 0.92 | 0.91 | 0.79 | 0.99 |
| Dora Baltea | Tavagnasco | ITA | 59 | 3313 | 1563 | 0.82 | 0.89 | 0.89 | 0.81 | 0.94 |
| Duero | Herrera de Duero | ESP | 63 | 12 740 | 525 | 0.78 | 0.96 | 0.94 | 0.8 | 1 |
| Ebro | Zaragoza | ESP | 63 | 40 434 | 679 | 0.85 | 0.84 | 0.85 | 0.84 | 0.96 |
| Elbe | Decin | CZ | 88 | 51 123 | 665 | 0.82 | 0.9 | 0.94 | 0.73 | 0.99 |
| Elbe | Dresden | DE | 157 | 53 096 | 664 | 0.79 | 0.88 | 0.87 | 0.74 | 0.99 |
| Emme | Emmenmatt | CH | 98 | 443 | 1288 | 0.77 | 0.75 | 0.79 | 0.7 | 0.84 |
| Fulda | Guntershausen | DE | 89 | 6366 | 793 | 0.78 | 0.84 | 0.82 | 0.73 | 0.97 |
| Fusta | Fustvatn | NO | 100 | 520 | 1868 | 0.71 | 0.74 | 0.84 | 0.64 | 0.95 |
| Glama | Elverum | NO | 127 | 15 426 | 646 | 0.69 | 0.79 | 0.73 | 0.6 | 0.97 |
| Gudena | Aastedbro | DK | 100 | 187 | 789 | 0.76 | 0.85 | 0.86 | 0.71 | 0.97 |
| Iller | Kempten | DE | 80 | 955 | 1087 | 0.72 | 0.76 | 0.79 | 0.64 | 0.88 |
| La Loire | Montjean | FR | 128 | 110 000 | 751 | 0.77 | 0.96 | 0.91 | 0.76 | 1 |
| Lapuanjoki | Keppo | FI | 81 | 3949 | 567 | 0.77 | 0.95 | 0.77 | 0.71 | 1 |
| Lindholm A | Elkaer Bro | DK | 101 | 106 | 649 | 0.76 | 0.83 | 0.76 | 0.71 | 0.97 |
| Lygna | Tingvatn | NO | 86 | 266 | 1699 | 0.69 | 0.75 | 0.71 | 0.6 | 0.94 |
| Maalselv | Malangsfoss | NO | 101 | 3239 | 612 | 0.71 | 0.75 | 0.59 | 0.58 | 0.95 |
| Main | Wuerzburg | DE | 185 | 14 031 | 676 | 0.78 | 0.84 | 0.79 | 0.74 | 0.96 |
| Neckar | Plochingen | DE | 91 | 3995 | 860 | 0.79 | 0.83 | 0.9 | 0.75 | 0.93 |
| Oder | Bohumin | CZ | 92 | 4665 | 742 | 0.74 | 0.78 | 0.76 | 0.67 | 0.93 |
| Otta | Lalm | NO | 87 | 3982 | 1006 | 0.68 | 0.7 | 0.82 | 0.6 | 0.95 |
| Rhine | Koeln | DE | 194 | 144 232 | 878 | 0.78 | 0.93 | 0.86 | 0.73 | 1 |
| Severn | Bewdley | GB | 135 | 4325 | 916 | 0.74 | 0.79 | 0.68 | 0.64 | 0.95 |
| Stura di Lanzo | Lanzo | ITA | 68 | 582 | 1279 | 0.74 | 0.72 | 0.76 | 0.73 | 0.86 |
| Tanaro | Farigliano | ITA | 68 | 1522 | 871 | 0.75 | 0.82 | 0.79 | 0.74 | 0.88 |
| Tanaro | Montecastello | ITA | 68 | 7985 | 881 | 0.73 | 0.78 | 0.78 | 0.76 | 0.88 |
| Thames | Kingston | GB | 81 | 9948 | 685 | 0.84 | 0.97 | 0.91 | 0.78 | 1 |
| Uggerby A | Asted Bro | DK | 97 | 151 | 651 | 0.75 | 0.77 | 0.73 | 0.7 | 0.94 |
| Vah | Sala | SK | 107 | 11 218 | 925 | 0.77 | 0.82 | 0.83 | 0.69 | 0.94 |
| Vils | Pfronten Ried | DE | 98 | 110 | 1090 | 0.7 | 0.75 | 0.78 | 0.64 | 0.88 |
| Vosso | Bulken | NO | 121 | 1102 | 2096 | 0.73 | 0.77 | 0.71 | 0.67 | 0.94 |
| Weser | Intschede | DE | 152 | 37 720 | 737 | 0.83 | 0.91 | 0.91 | 0.79 | 0.96 |

## APPENDIX B. HURST COEFFICIENT ESTIMATION METHODS

### RESCALED RANGE STATISTICS

Assume observation time series of length N and let $Y(n) = \sum_{i=1}^{n} X_i$ be a series of partial sums of the runoff time series $X_t$.

Then, the rescaled range $R/S(n)$ (Hurst, 1951) is defined as

$$R/S(n) = \frac{\max_{0\le t\le n}(Y(t) \quad - \frac{t}{n}Y(n)) - \min_{0\le t\le n}(Y(t) - \frac{t}{n}Y(n))}{\left(\frac{1}{n}\sum_{i=1}^{n}X_i^2 - \frac{1}{n^2}Y(n)^2\right)^{1/2}} \tag{7}$$

In case of long memory

$$E(R/S(n)) \sim Cn^H \quad \text{as} \quad n \to \infty \tag{8}$$

where $C$ is a constant, $n$ is the number of observations, and $H$ is the Hurst coefficient.

By taking the logarithm of Equation (8), we obtain

$$\ln\left(E\left(\frac{R(n)}{S(n)}\right)\right) = H\ln(n) + \ln(C) \tag{9}$$

Now, let us consider a subdivision of the time series into $K$ blocks of size $N/K$, and let $k_i = iN/K$ be the starting points of each block. In order to obtain the estimator of $H$, Equation (7) is first evaluated for each $n$ and $k_i$ as far as $k_i + n \le N$, thus obtaining a series $R(k_i,n)/S(k_i,n)$ for each starting point $k_i$ and for each length textitn. The Hurst coefficient estimate is then given by the slope of a regression line between $ln(n)$ and the logarithm of the rescaled range $R(k_i,n)/S(k_i,n)$.

According to Teverovsky *et al*. (1995), the 'low end' of the plot is not suitable for estimation, since any possible short range dependence in the time series would result in a 'transient zone' (as described in Salas *et al*., 1979) in this area. The very high end of the plot is not suited either, since here too few points are present to make 'reliable estimates'. For this reason, we estimated the Hurst coefficient only from the $R(k_i,n)/S(k_i,n)$ from the central part of the plot (Montanari *et al*., 1997).

### REGRESSION ON THE PERIODOGRAM

Geweke and Porter-Hudak (1983) showed, that when considering the periodogram of the time series given by

$$I(\lambda) = \frac{1}{2\pi N}\left|\left(\sum_{j=0}^{N-1}X_j e^{-ij\lambda}\right)\right|^2 \quad \left\{\omega = \frac{2\pi k}{N}; \forall k = 1,\ldots,T\right\} \tag{10}$$

where $T = u_l\left\lfloor\frac{n-1}{2}\right\rfloor$, $\lambda$ are the frequencies, the following equation holds:

$$\ln(I(\lambda)) \sim c - d\ln\left(4\sin^2(\lambda/2)\right) \tag{11}$$

where $c$ is a constant (dependent on the variance of the time series).

Thus, fitting a regression line on the logarithm of the frequencies and logarithm of the periodogram delivers an estimate for $d$ with $d = 1 - 2H$. $T$ gives the upper limit for the frequencies used in the regression. As suggested in Taqqu and Teverovsky (1998), we use $u_l = 0, 1$, i.e. the bottom 10% of the frequencies.

### WHITTLE ESTIMATOR

The Whittle estimator is a likelihood-based method from the frequency domain. The Hurst coefficient is obtained by minimizing the function

$$Q(H) = \int_{-\pi}^{\pi}\frac{I(\lambda)}{f(\lambda,H)}d\lambda \tag{12}$$

where $I(\lambda)$ is defined as in Equation (10) and $f(\lambda,H)$ is the spectral density. While performing the actual minimization, Equation (12) is discretized to Beran (1994)

$$Q(H) = \sum_{j=1}^{[(N-1)/2]}\frac{I(\lambda_j)}{f(\lambda_j,H)} \tag{13}$$

and it is assumed that the data follows either a fractionally integrated moving average process $ARFIMA(p,d,q)$ or a fractional Gaussian noise (with $d = H - 0.5$). We assumed an $ARFIMA(p,d,q)$ process.

The parameters $p, q$ were obtained by fitting a $ARFIMA(p,d,q)$ model to some of the runoff series for all combinations of the parameters based on the (partial) autocorrelation function. We then selected the most appropriate model based on the minimum of the Akaike criterion. Since the choice of $p = 1, q = 1$ was suitable for the series analyzed, we used these parameters for all time series in the study.

For the Whittle estimator, construction of confidence intervals is possible. We constructed 95% confidence intervals as $(H - 1.96(V/N)^{0.5}, H + 1.96(V/N)^{0.5})$. Where $V = 2D^{-1}$ with $D_{ij} = 1/2\pi\int_{-\pi}^{\pi}\frac{\partial}{\partial\theta_i}logf(\lambda)\frac{\partial}{\partial\theta_j}logf(\lambda)d\lambda$ is the estimator of variance obtained from Equation (13) (Rosse, 1996).

### AGGREGATED VARIANCE

Consider the averaged aggregated series

$$X_i^k = \frac{1}{k}\sum_{l=(i-1)k+1}^{ik}X_l \qquad i = 1,2,\ldots\lfloor N/k\rfloor \tag{14}$$

Then, the variance of this series is estimated by

$$\widehat{Var}X^{(k)} = \frac{\sum_{i=l}^{N/k}\left(X_l^{(k)} - \bar{X}\right)^2}{N/k} \tag{15}$$

One plots the logarithm of the variances (Equation (15)) of the aggregated series (Equation (14)) against the respective aggregation length $k$. The points so obtained should lie on a straight line with slope 2H-2 from which $H$

was estimated by regression. Only the central region of the plot was considered in the regression, since the short range dependencies affect the low end of the plot and an insufficient number of blocks affects the high end of the plot (Teverovsky *et al.*, 1995).

### LSV

Another method in the temporal domain is the LSV method (Tyralis and Koutsoyiannis, 2011). LSV estimates $H$ and the variance of the time series simultaneously, offering an unbiased estimator of both parameters, if the assumption of self-similarity and normal distribution of the data is fulfilled. The method is based on an unbiased estimator of the variance of $X_n$ for long range-dependent time series derived in Beran (1994). Denote $\gamma_\tau = Cov[X_t, X_{t+\tau}]$ the autocovariance function of $X_t$. Then, based on

$$E\left(S^2\right) = \frac{N - 1 - 2\sum_{k=1}^{N-1}(1 - k/N)\rho_k}{N - 1}\gamma_0. \tag{16}$$

and on the property of the series $Z^{(k)}$

$$Var\left(Z^{(k)}\right) = k^{2H}\gamma_0 \tag{17}$$

one obtains a bias for the variance estimate on all scales (depending on $H$):

$$E\left(S^{2(k)}\right) = \frac{N/k - (N/k)^{2H-1}}{N/k - 1}\gamma_0^k \tag{18}$$

Where $Z^{(k)}$ is defined as

$$Z_i^{(k)} = kX_i^{(k)} \tag{19}$$

and $S^{2(k)}$

$$S^{2(k)} = \frac{\sum_{i=1}^{N/k}\left(Z_i^{(k)} - \bar{Z}_i^{(N)}\right)^2}{N/k - 1} \tag{20}$$

By minimizing an error function

$$e^2\left(\sigma^2, H\right) = \sum_{k=1}^{[n/10]} \frac{\left(E\left(S^{2(k)}\right) - s^{2(k)}\right)^2}{k^p} \tag{21}$$

(which is done numerically) one obtains the estimate for $H$. This method furthermore allows a graphical depiction of the standard deviation against all scales (a climacogram Koutsoyiannis, 2010), thus providing a way to visually verify the validity of the scaling law for each scale.